

AperTO - Archivio Istituzionale Open Access dell'Università di Torino

## Phototransformation of the Herbicide Propanil in Paddy Field Water

### **This is the author's manuscript**

*Original Citation:*

*Availability:*

This version is available <http://hdl.handle.net/2318/1637862> since 2017-05-24T12:05:43Z

*Published version:*

DOI:10.1021/acs.est.6b05053

*Terms of use:*

Open Access

Anyone can freely access the full text of works made available as "Open Access". Works made available under a Creative Commons license can be used according to the terms and conditions of said license. Use of all other works requires consent of the right holder (author or publisher) if not exempted from copyright protection by the applicable law.

(Article begins on next page)

This is the author's final version of the contribution published as:

Carena, Luca; Minella, Marco; Barsotti, Francesco; Brigante, Marcello;  
Milan, Marco; Ferrero, Aldo; Berto, Silvia; Minero, Claudio; Vione, Davide.  
Phototransformation of the Herbicide Propanil in Paddy Field Water.  
ENVIRONMENTAL SCIENCE & TECHNOLOGY. 51 (5) pp: 2695-2704.  
DOI: 10.1021/acs.est.6b05053

The publisher's version is available at:

<http://pubs.acs.org/doi/pdf/10.1021/acs.est.6b05053>

When citing, please refer to the published version.

Link to this full text:

<http://hdl.handle.net/2318/1637862>

## Phototransformation of the herbicide propanil in paddy field water

Luca Carena,<sup>a</sup> Marco Minella,<sup>a</sup> Francesco Barsotti,<sup>a</sup> Marcello Brigante,<sup>b</sup> Marco Milan,<sup>c</sup> Aldo Ferrero,<sup>c</sup> Silvia Berto,<sup>a</sup> Claudio Minero,<sup>a</sup> Davide Vione<sup>a,d,\*</sup>

<sup>a</sup> Dipartimento di Chimica, Università di Torino, Via Pietro Giuria 5, 10125 Torino, Italy. <http://www.chimicadellambiente.unito.it>

<sup>b</sup> Clermont Université, Université Blaise Pascal, Institut de Chimie de Clermont-Ferrand, & CNRS, UMR 6296, ICCF, BP 80026, F-63177 Aubière, France.

<sup>c</sup> Dipartimento di Scienze Agrarie, Forestali e Alimentari, Università di Torino, Largo Paolo Braccini 2, 10095 Grugliasco (TO), Italy.

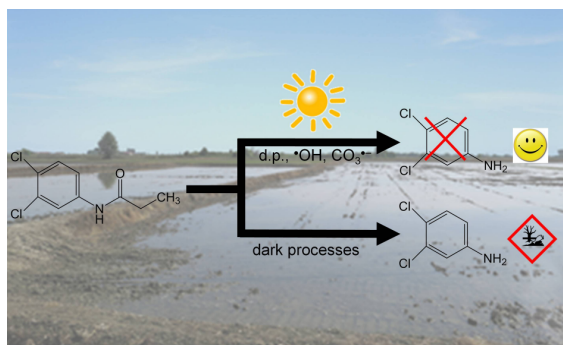
<sup>d</sup> Università di Torino, Centro Interdipartimentale NatRisk, Largo Paolo Braccini 2, 10095 Grugliasco (TO), Italy. <http://www.natrisk.org>

\* Corresponding author. Phone: +39-011-6705296; Fax: +39-011-6705242.

E-mail: [davide.vione@unito.it](mailto:davide.vione@unito.it)

### Abstract

When irradiated in paddy-field water, propanil (PRP) undergoes photodegradation by direct photolysis, by reactions with  $\bullet\text{OH}$  and  $\text{CO}_3^{\bullet-}$ , and possibly also with the triplet states of chromophoric dissolved organic matter. Irradiation also inhibits the non-photochemical (probably biological) degradation of PRP. The dark and light-induced pathways can be easily distinguished because 3,4-dichloroaniline (34DCA, a transformation intermediate of considerable environmental concern) is produced with almost 100% yield in the dark but not at all through photochemical pathways. This issue allows an easy assessment of the dark process(es) under irradiation. In the natural environment we expect PRP photodegradation to be important only in the presence of elevated nitrate and/or nitrite levels, e.g.,  $[\text{NO}_3^-]$  approaching  $1 \text{ mmol L}^{-1}$  (corresponding to approximately  $60 \text{ mg L}^{-1}$ ). Under these circumstances,  $\bullet\text{OH}$  and  $\text{CO}_3^{\bullet-}$  would play a major role in PRP phototransformation. Because flooded paddy fields are efficient denitrification bioreactors that can achieve decontamination of nitrate-rich water used for irrigation, irrigation with such water would both enhance PRP photodegradation and divert PRP dissipation processes away from the production of 34DCA, at least in the daylight hours.



## Introduction

Propanil (N-(3,4-Dichlorophenyl)propanamide, hereafter PRP) is a post-emergence contact herbicide that is widely used in rice cultivation. It acts as an inhibitor of photosynthesis by blocking the electron-transfer processes involved in CO<sub>2</sub> reduction, killing weeds that, differently from rice, do not carry out fast PRP hydrolysis to 3,4-dichloroaniline (34DCA) with the enzyme aryl acylamidase.<sup>1</sup> PRP is not very toxic to mammals,<sup>2</sup> but potentially lethal human poisoning during pesticide use may occasionally occur. Indeed, both PRP and its major metabolite 34DCA can cause methaemoglobinaemia.<sup>3</sup> PRP is a pollutant of concern for aquatic organisms such as crustaceans (acute toxic effects detected at mg L<sup>-1</sup> levels)<sup>4</sup> and, most notably, algae (acute toxicity at tens µg L<sup>-1</sup> levels)<sup>4</sup> and some fish (LC<sub>50</sub> levels in the range of tens µg L<sup>-1</sup> to tens mg L<sup>-1</sup> depending on the species).<sup>5,6</sup> PRP undergoes relatively fast degradation in paddy water, and 34DCA is a major transformation intermediate that shows comparable or even longer persistence than the parent compound.<sup>7,8</sup> Similarly to PRP, 34DCA is acutely toxic at mg L<sup>-1</sup> levels to fish, crustaceans and algae,<sup>2</sup> but it can also interfere with the development of fish embryos and with the reproduction of crustaceans at µg L<sup>-1</sup> levels.<sup>9-11</sup> Both PRP and 34DCA show some genotoxic effects, but none of them is classified as carcinogenic.<sup>2</sup>

The transformation of PRP into 34DCA is known to take place during PRP biological degradation, but it could also occur under some irradiation conditions.<sup>12,13</sup> The persistence of the parent compound and of its main metabolite suggests that a water-holding period of several days after PRP spraying and before water discharge would minimise environmental contamination phenomena by either PRP or 34DCA.<sup>7,8</sup> The cited environmental effects have urged the introduction of some restrictions to PRP use in the US,<sup>14</sup> and in the EU its use is permitted only under emergency conditions.<sup>15</sup> However, PRP is still manufactured and applied on a large scale worldwide.<sup>16</sup>

Several studies have focused on PRP biodegradation as the supposed main transformation pathway in paddy-field water.<sup>17</sup> However, PRP also undergoes photodegradation under sunlight<sup>17</sup> and the kinetics of phototransformation might be comparable with those of biochemical transformation and with the overall field persistence.<sup>13</sup> Unfortunately, to date the photochemical degradation of PRP has been studied either in synthetic solutions (ultra-pure water),<sup>13,18</sup> or upon irradiation of natural waters but without a distinction between direct and indirect photolysis processes, which prevents a generalisation of laboratory results to field conditions.<sup>19</sup>

The direct photolysis occurs when a compound (e.g. a xenobiotic) absorbs sunlight and undergoes transformation. In contrast, indirect photochemistry is triggered by the absorption of sunlight by photoactive water components (photosensitisers) such as chromophoric dissolved organic matter (CDOM), nitrate and nitrite. Sunlight absorption by photosensitisers induces the generation of a number of reactive transient species. In particular, nitrate and nitrite produce hydroxyl radicals ( $\bullet\text{OH}$ ). Irradiated CDOM yields  $\bullet\text{OH}$  through multiple reaction pathways, as well as reactive triplet states ( $^3\text{CDOM}^*$ ) that can also react with dissolved oxygen to produce singlet oxygen ( $^1\text{O}_2$ ) as an additional transient. Moreover, oxidation of carbonate and bicarbonate by  $\bullet\text{OH}$  and of carbonate by  $^3\text{CDOM}^*$  yields the carbonate radical,  $\text{CO}_3^{\bullet-}$ . These transients are quickly scavenged or deactivated soon after formation, and their reaction with xenobiotics is usually a secondary decay pathway. Indeed,  $\bullet\text{OH}$  mainly reacts with natural dissolved organic matter (DOM, not necessarily chromophoric) and, to a lesser extent, with carbonate and bicarbonate;  $\text{CO}_3^{\bullet-}$  is mainly scavenged by DOM,  $^1\text{O}_2$  is mostly inactivated to ground-state (triplet)  $\text{O}_2$  by collision with water, and  $^3\text{CDOM}^*$  react with  $\text{O}_2$  or undergo internal conversion with heat dissipation.<sup>20-25</sup>

The goal of this paper is to address the photochemical degradation of PRP in paddy-field water, highlighting the importance of the different phototransformation pathways. Due to poor knowledge about the photochemistry of irradiated paddy water, the photogenerated transient species were also quantified in paddy-water samples. The understanding of paddy-water photochemistry is important

both to get insight into the fate of PRP and other pesticides, and to assess the overall processing of, e.g., arsenic species in paddy fields.<sup>27</sup>

## Experimental

**Rice fields under study.** The paddy water used in the present study was collected in three farms located in the municipalities of Rovasenda (45.536970° N; 8.298246° E, 220 m a.s.l), Santhià (45.377806° N; 8.201165° E, 179 m a.s.l) and San Germano Vercellese (S.GermanoVC; 45.356445° N; 8.244346° E; 165m a.s.l), in the province of Vercelli, Piemonte region, NW Italy. The rice field size was 0.9 ha, 1.1 ha and 0.7 ha in Santhià, S.GermanoVC and Rovasenda, respectively. These sites are included in the most important rice growing area of Italy, where over 90% of the total Italian rice is grown. Further details, including the relationship between rice plant height and radiation transmittance, are reported as Supporting Information (hereafter SI).

Sampling took place in late May, 2016. Two one-liter glass bottles (Duran, Mainz, Germany) were filled starting from a bulk of 10 L paddy water collected in each rice field, by randomly filling a 10 L PTFE bucket. Samples were temporarily stored in a portable refrigerator till transfer to the laboratory, where they were vacuum filtered (polyamide filters, 0.45 µm pore size, Sartorius) and kept refrigerated (5.5 °C) until analysis or irradiation. At the time of sampling, the water level in each paddy field was around 5-7 cm and the crop was at 3-4 leaf stage (growth stage 13-14 on the BBCH scale).<sup>28</sup> At this stage the rice plants do not yet produce an important shading of the paddy water, but later growth causes a considerable decrease of the light transmitted through the rice canopy (see **Figure S1**(SI)).

**Irradiation experiments.** Solutions to be irradiated (5 or 20 mL total volume) were placed in cylindrical Pyrex glass cells (having a lateral neck for sample transfer, and tightly closed with a screw cap), and placed under the chosen lamp (*vide infra*) for irradiation under magnetic stirring. The solutions were irradiated mainly from the top. After the scheduled irradiation time, the whole

solutions (5-mL case) or 1.2 mL solution aliquots (20-mL case) underwent analysis. The temperature of the irradiated solutions was  $\sim 30^{\circ}\text{C}$ . Pictures of the home-made irradiation set-up are provided as SI, **Figure S2**(SI).

Paddy water samples (20 mL, *vide infra*) were irradiated under a lamp spanning a wide spectral emission range, with the purpose of measuring the formation rates of  $\bullet\text{OH}$ ,  $^1\text{O}_2$  and  $^3\text{CDOM}^*$ . The determination of the photochemical kinetics parameters of PRP (direct photolysis quantum yield and second-order reaction rate constants) involved experiments with systems based on ultra-pure water instead of paddy water (5 mL total volume), irradiated with lamps that were chosen to achieve selective excitation of the photoactive compounds. In these experiments, the standard initial concentration of PRP was  $20\ \mu\text{mol L}^{-1}$ , or less when required by the kinetic determinations. For instance, the reaction between PRP and  $\bullet\text{OH}$  was studied using nitrate photolysis as  $\bullet\text{OH}$  source and competition kinetics with 2-propanol as  $\bullet\text{OH}$  scavenger.<sup>29</sup> The relevant solutions were irradiated under a 20 W Philips TL01 lamp, having an emission maximum at 313 nm and producing a  $4.1\pm 0.1\ \text{W m}^{-2}$  UV irradiance on top of the irradiated systems. The UV irradiance (290-400 nm) was measured with an irradiance meter by CO.FO.ME.GRA. (Milan, Italy). The same lamp was used to study the direct photolysis of PRP. The reaction between PRP and the triplet state of anthraquinone-2-sulphonate ( $^3\text{AQ2S}^*$ ) was studied using a UVA black lamp (Philips TL-D 18 W, emission maximum at 368 nm), producing a UV irradiance of  $27.5\pm 0.6\ \text{W m}^{-2}$  on top of the irradiated systems. AQ2S was chosen as CDOM proxy for experimental convenience, as it is virtually the only triplet sensitizer that allows a straightforward determination of the triplet-state reaction rate constant by using steady irradiation alone.<sup>30</sup> Unfortunately,  $^3\text{AQ2S}^*$  is sometimes more reactive than average  $^3\text{CDOM}^*$ ,<sup>31</sup> thus additional rate constants of PRP triplet sensitisation were obtained by using the laser flash photolysis technique (*vide infra*). The reaction between PRP and  $^1\text{O}_2$  was studied using Rose Bengal as  $^1\text{O}_2$  source, irradiating the solutions with a 18 W Philips TLD Yellow lamp with emission maximum at 545 nm. The emission spectra of the lamps were obtained with an

Ocean Optics USB 2000 CCD spectrophotometer, and corrected for the transmittance of the Pyrex window of the irradiation cells. Based on these data, the actual spectral photon flux density of the lamps was obtained by chemical actinometry using 2-nitrobenzaldehyde (NBA). The detailed procedure for NBA actinometry is described elsewhere.<sup>32</sup> Because the Yellow lamp does not allow for NBA actinometry, its spectral photon flux density was calculated by taking into account the shape of the emission spectrum, the integral irradiance measured with a Testo 540 irradiance meter, the irradiation geometry and the solution volume. The photon flux density thus obtained was only approximate, but that did not affect the measurement of the  $^1\text{O}_2$  reaction rate constant. Indeed, the formation rate of  $^1\text{O}_2$  by irradiated Rose Bengal ( $R_{^1\text{O}_2}^{\text{RB}}$ ) was measured independently with furfuryl alcohol (FFA) as a probe molecule, and only  $R_{^1\text{O}_2}^{\text{RB}}$  was used in rate-constant calculations (see SI). The spectral photon flux densities of the used lamps and the absorption spectra of the photosensitisers are reported in **Figure S3**(SI). The time evolution of PRP was monitored by liquid chromatography (see SI for instrumental details and elution conditions). The same technique was used to monitor the time trend of the photochemical probe molecules added to paddy water (*vide infra*).

The used chemicals were of analytical grade, and organic solvents were of gradient grade. They were used as obtained, without further purification. Ultra-pure water was produced with a Milli-Q<sup>TM</sup> system (Millipore).

### **Measurement of photoinduced transients upon irradiation of paddy-field water.**

Probe molecules were used to measure the photogeneration of transient species.<sup>33</sup> The paddy water samples (20 mL) were put inside the irradiation cells, spiked with each probe molecule separately (added as pure solid or liquid and let dissolve) and irradiated under a 40 W Philips TL K05 lamp, with emission maximum at 365 nm. This lamp spans the UVB, UVA and visible wavelength intervals and its spectral photon flux density is reported in **Figure S4**(SI), together with the



absorption spectra of the irradiated water samples. Dark experiments on paddy water were carried out under the same irradiation device, by wrapping the cells with aluminium foil. Previous results suggest that the probe molecules used in this work (2,4,6-trimethylphenol, furfuryl alcohol and benzene) do not directly photolyse under the TL K05 lamp (i.e., they are not degraded upon irradiation in ultra-pure water), basically because they do not absorb lamp radiation significantly.<sup>34</sup> The formation of  $^3\text{CDOM}^*$  was assessed by using 2,4,6-trimethylphenol (TMP) as probe molecule, that of  $^1\text{O}_2$  by using furfuryl alcohol (FFA), and that of  $\bullet\text{OH}$  with the transformation reaction of benzene into phenol (with assumed yield  $\eta = 0.7$ ).<sup>35-44</sup> Based on previous studies and literature references,<sup>35-44</sup> the SI reports details concerning experimental and calculation procedures to determine the formation rates of  $^3\text{CDOM}^*$  and  $^1\text{O}_2$  from CDOM ( $R_{^3\text{CDOM}^*}$  and  $R_{^1\text{O}_2}$ , respectively), the formation rates of total  $\bullet\text{OH}$  and of  $\bullet\text{OH}$  generated by CDOM ( $R_{\bullet\text{OH}}^{\text{tot}}$  and  $R_{\bullet\text{OH}}^{\text{CDOM}}$ , respectively), as well as the steady-state concentrations [ $^3\text{CDOM}^*$ ], [ $^1\text{O}_2$ ] and [ $\bullet\text{OH}$ ].

With  $R_{^3\text{CDOM}^*}$ ,  $R_{^1\text{O}_2}$  and  $R_{\bullet\text{OH}}^{\text{CDOM}}$  one can assess the quantum yields of transients photogeneration by irradiated CDOM, using the lamp photon flux absorbed by CDOM itself,  $P_a^{\text{CDOM}}$ :

$$P_a^{\text{CDOM}} = \int_{\lambda} p^{\circ}(\lambda)(1 - 10^{-A_1(\lambda)b}) d\lambda \quad (4)$$

where  $p^{\circ}(\lambda)$  is the spectral photon flux density of the lamp,  $A_1(\lambda)$  the water sample absorbance over an optical path length of 1 cm, and  $b = 1.6$  cm the optical path length inside the irradiated solutions. The quantum yields are calculated as follows:  $\Phi_{^3\text{CDOM}^*} = R_{^3\text{CDOM}^*} (P_a^{\text{CDOM}})^{-1}$ ,  $\Phi_{^1\text{O}_2} = R_{^1\text{O}_2} (P_a^{\text{CDOM}})^{-1}$  and  $\Phi_{\bullet\text{OH}}^{\text{CDOM}} = R_{\bullet\text{OH}}^{\text{CDOM}} (P_a^{\text{CDOM}})^{-1}$ . Note that CDOM is by far the main light absorber in natural waters between 300 and 500 nm,<sup>45</sup> which is quite in the range of the used lamp.

The TL K05 lamp was also used to assess the photochemical degradation of PRP in irradiated paddy water. In these experiments, 20  $\mu\text{mol L}^{-1}$  PRP was spiked to 20 mL paddy water before irradiation.

**Kinetic data treatment.** The degradation of a given substrate S (PRP or probe molecule) was fitted with a pseudo-first order kinetic equation of the form  $C_t^S = C_o^S e^{-k_d^S t}$ , where  $C_t^S$  is the concentration of S at the time t,  $C_o^S$  the initial concentration and  $k_d^S$  the pseudo-first order degradation rate constant. The initial transformation rate of S is  $R_o^S = k_d^S C_o^S$ . The time evolution of phenol formed from benzene (used to measure  $\bullet\text{OH}$  photogeneration) was fitted with  $C_t^P = \frac{k_f^P C_o^B}{k_d^B - k_d^P} (e^{-k_d^P t} - e^{-k_d^B t})$ , where  $C_o^B$  and  $k_d^B$  are the initial concentration and the pseudo-first order degradation rate constant of benzene, respectively,  $C_t^P$  is the concentration of phenol at the time t, and  $k_f^P$  and  $k_d^P$  are, respectively, the pseudo-first order formation and degradation rate constants of phenol. The initial phenol formation rate is  $R_o^P = k_f^P C_o^B$ . Note that  $\eta = k_f^P (k_d^B)^{-1} = 0.7$  is the formation yield of phenol from benzene.

In some dark runs PRP had an initial lag time before the onset of degradation, which is usually associated with biological processes.<sup>46</sup> In these cases the PRP time trend was successfully fitted with the following equation:<sup>47</sup>

$$C_t = C_o e^{-kt} \frac{e^{kL}}{1 + (e^{kL} - 1) e^{-kt}} \quad (5)$$

where  $C_t$  is PRP concentration at the time t,  $C_o$  its initial concentration, L the lag time, and k the pseudo-first order rate constant of PRP degradation.

**Chemical and spectroscopic characterisation of paddy-field water.** The absorption spectra were measured with a Varian Cary 100 Scan double-beam UV-visible spectrophotometer, using Hellma quartz cuvettes with 1 cm optical path length (see **Figure S4**(SI)). The fluorescence excitation-emission matrix (EEM) spectra were taken with a Cary Eclipse fluorescence

spectrofluorimeter, using 10 nm slit width on both excitation and emission and a 1 cm fluorescence quartz cuvette.

The inorganic cations ( $\text{Ca}^{2+}$ ,  $\text{Mg}^{2+}$ ,  $\text{Na}^+$ ,  $\text{K}^+$ ,  $\text{NH}_4^+$ ) were determined with a Dionex DX 500 ion chromatograph, equipped with Rheodyne injector (20  $\mu\text{L}$  sample loop), LC-30 chromatography oven (operated at 30 °C), GP-40 pump for low-pressure gradients, Dionex IonPac CG-12A guard column (4  $\times$  50 mm), Dionex IonPac CS12A column (4  $\times$  250 mm), CERS 500 electrochemical suppression unit, and ED-40 conductometric detector. The eluent was a 20 mmol  $\text{L}^{-1}$  solution of methanesulphonic acid at 1 mL  $\text{min}^{-1}$  flow rate.

Inorganic anions ( $\text{Cl}^-$ ,  $\text{NO}_3^-$ ,  $\text{SO}_4^{2-}$ ) were determined with the same instrument as above, equipped with Dionex IonPac AG9-HC guard column (4  $\times$  50 mm), Dionex IonPac AS9-HC column (4  $\times$  250 mm) and ASRS 300 electrochemical suppression unit. The eluent was a 9 mmol  $\text{L}^{-1}$  solution of  $\text{K}_2\text{CO}_3$  at 1 mL  $\text{min}^{-1}$  flow rate.

Nitrite was determined by pre-column derivatisation with 2,4-dinitrophenylhydrazine to produce the corresponding azide in acidic solution (10 min reaction time; the solution of the derivatising agent in water + HCl +  $\text{CH}_3\text{CN}$  was previously purified by extraction with  $\text{CCl}_4$ ).<sup>48</sup> The derivatised sample was analysed by liquid chromatography using a reverse-phase  $\text{C}_{18}$  column (see SI for instrumental details), eluting with a 50:50 mixture of acetonitrile and water (pH 3 by  $\text{H}_3\text{PO}_4$ ) at 1 mL  $\text{min}^{-1}$  flow rate, and using 305 nm as quantification wavelength. Under these conditions, the retention time of the azide was 4.2 min.

The dissolved organic carbon (DOC) was determined as the difference between total (dissolved) carbon (TC) and inorganic carbon (IC), using a Shimadzu TOC-VCSH instrument. The TOC analyser was equipped with an ASI-V autosampler and a TNM-1 module for the measurement of total nitrogen (TN), which was determined as well. The pH of the samples was measured with a combined glass electrode connected to a Metrohm 602 pH meter.

**Laser flash photolysis experiments.** Flash photolysis runs were carried out using the third harmonic (355 nm) of a Quanta Ray GCR 130-01 Nd:YAG laser system instrument, used in a right-angle geometry with respect to the monitoring light beam. The single pulses energy was set to 35 mJ. A 3 mL solution volume was placed into a quartz cuvette (path length of 1 cm) and used for a maximum of four consecutive laser shots, to avoid interference by phototransformation products. The transient absorbance at the pre-selected wavelength was monitored by a detection system consisting of a pulsed xenon lamp (150 W), monochromator and a photomultiplier (1P28). A spectrometer control unit was used for synchronising the pulsed light source and programmable shutters with the laser output. The signal from the photomultiplier was digitised by a programmable digital oscilloscope (HP54522A). A 32 bits RISC-processor kinetic spectrometer workstation was used to analyse the digitised signal.

The triplet sensitisation of PRP was studied using CDOM proxies such as 1-nitronaphthalene (1NN, 45.5  $\mu\text{mol L}^{-1}$ ), anthraquinone-2-sulphonate (AQ2S, 75.4  $\mu\text{mol L}^{-1}$ ), riboflavin (RF, 26.8  $\mu\text{mol L}^{-1}$ ) and 4-carboxybenzophenone (CBBP, 185  $\mu\text{mol L}^{-1}$ ), under conditions chosen on the basis of previous studies.<sup>30,49-51</sup> These compounds are well known triplet sensitisers under 355 nm laser excitation. The triplet decay was monitored at different PRP concentration values, and the measured pseudo-first order decay constant  $k_{\text{Sens}}$  was plotted as a function of PRP concentration. The latter was varied within a maximum range of 0.05-1.25 mM, depending on the effect of PRP addition on  $k_{\text{Sens}}$ . The slopes of linearly fitted  $k_{\text{Sens}}$  vs. [PRP] data were used to obtain the second-order quenching rate constants between PRP and the photosensitiser triplet states ( $^3\text{1NN}^*$ ,  $^3\text{AQ2S}^*$ ,  $^3\text{RF}^*$ , and  $^3\text{CBBP}^*$ ), according to a Stern-Volmer approach.

**Photochemical modelling.** The photodegradation of PRP in paddy water was also assessed with the APEX software (Aqueous Photochemistry of Environmentally-occurring Xenobiotics).<sup>52</sup> APEX predicts photochemical reaction kinetics from photoreactivity parameters (absorption spectra, direct photolysis quantum yields and second-order reaction rate constants of a xenobiotic

with the main photochemically produced transient species, formation quantum yields and decay kinetics of photoreactive transients), and from data of water chemistry and depth. The photoreaction pathways modelled by APEX include the direct photolysis and the reaction with the transients  $\bullet\text{OH}$ ,  $^1\text{O}_2$ ,  $\text{CO}_3^{\bullet-}$  and  $^3\text{CDOM}^*$ . In this work chemical and photochemical paddy-water data, as well as PRP photoreactivity parameters were used for modelling. The used solar spectrum is referred to late May - early June at mid latitude,<sup>53</sup> when PRP is applied to paddy fields in the studied area and the water depth is around 5 cm.<sup>8</sup> The modelled lifetimes are referred to actual 24-h days (the day-night cycle is taken into account) under fair weather in the relevant season.

## Results and Discussion

**PRP photochemical reactivity.** The reactivity of PRP by direct photolysis and with  $\bullet\text{OH}$ ,  $^1\text{O}_2$  and AQ2S triplet state ( $^3\text{AQ2S}^*$ ) was assessed by means of steady irradiation experiments. The relevant measurements followed an already established protocol<sup>26,31,50</sup> and the results are reported in the SI. The second-order rate constant for the reaction between PRP and  $\text{CO}_3^{\bullet-}$  is available from literature.<sup>54</sup> This and other photoreaction parameters are reported in **Table 1**. The main advantage when using AQ2S as CDOM proxy is experimental convenience, because AQ2S does not yield important levels of  $\bullet\text{OH}$  or  $^1\text{O}_2$  under irradiation and because its second-order rate constants of triplet sensitisation can be easily determined by steady irradiation.<sup>26,30,31,50</sup> The  $^3\text{AQ2S}^*$  rate constants can sometimes be surprisingly similar to those of natural  $^3\text{CDOM}^*$ ,<sup>26,55</sup> but in other cases overestimations are possible due to the higher reactivity of  $^3\text{AQ2S}^*$  compared to  $^3\text{CDOM}^*$ .<sup>56</sup> Additional photosensitisers were thus chosen, and in particular 1NN, RF and CBBP. RF and CBBP have several analogies with known CDOM components,<sup>57,58</sup> while the 1NN triplet state is less reactive than that of AQ2S and it is very conveniently studied by laser flash photolysis.<sup>49,56</sup> Indeed, the study of the reactivity of  $^3\text{1NN}^*$ ,  $^3\text{RF}^*$  and  $^3\text{CBBP}^*$  with PRP required the use of a laser apparatus, which was also used to measure again the second-order reaction rate constant between

PRP and  $^3\text{AQ2S}^*$ . It has been reported that the measured laser and steady-irradiation  $^3\text{AQ2S}^*$  second-order rate constants are very similar in the case of nitrobenzene,<sup>59,60</sup> but the laser apparatus might also detect physical quenching phenomena that do not lead to chemical reactions and are not taken into account by steady irradiation.<sup>61</sup> Moreover, in some cases the initial substrate is reformed during steady irradiation by a combination of oxidation and reduction processes.<sup>62,63</sup> The experimental laser flash photolysis data obtained in this work are summarised in **Figure S10(SI)**. In the case of PRP +  $^3\text{AQ2S}^*$ , the steady-irradiation (reaction) rate constant was actually an order of magnitude lower than the laser (quenching) one (see **Table 1**). In contrast, the  $^3\text{AQ2S}^*$  reaction rate constant was not much different from the quenching constants measured with the other photosensitisers.

**Figure S11(SI)** reports correlation plots of the measured rate constants of triplet sensitisation, with the triplet-state energy and with the triplet reduction potential.<sup>64</sup> The best correlation is obtained when taking the triplet energy into account, which might suggest that the reactions might at least partially involve an energy transfer from the sensitiser triplet states to PRP.<sup>64</sup> If an important fraction of the transferred energy is dissipated by e.g. internal conversion, that might explain the difference between the measured quenching and reaction rate constants in the case of AQ2S. As a starting hypothesis, a PRP triplet sensitisation rate constant of around  $10^8 \text{ L mol}^{-1} \text{ s}^{-1}$  was assumed hereafter. If the difference between the  $^3\text{AQ2S}^*$  quenching and reaction rate constants is due to back-reduction processes, or if important energy dissipation pathways are operational, there could be implications for the role of triplet-sensitised reactions in an environmental setting.<sup>62,63</sup>

The reactivity of PRP with  $^1\text{O}_2$  is very low, ending up with  $k_{\text{PRP},^1\text{O}_2} < 10^5 \text{ M}^{-1} \text{ s}^{-1}$ . This is near the lower end of the rate constant values that can be measured with the used methodology. For this reason the experimental data (see **Figure S6(SI)**), as well as the  $k_{\text{PRP},^1\text{O}_2}$  value thus obtained (see **Table 1**) are affected by a non-negligible uncertainty.

Negligible formation of 34DCA from PRP was detected in the irradiation experiments, while almost quantitative formation of 34DCA was observed in the dark at pH 8 or lower (see **Figure S12(SI)**). The time trend of PRP in the dark showed a clear lag time, which could suggest a biological process of PRP degradation<sup>46,47</sup> and would be consistent with the known PRP biodegradability.<sup>65,66</sup> The elevated formation yield of 34DCA from PRP observed in our dark experiments would be consistent with the known pathways of PRP biodegradation, too.<sup>7,8,12,13</sup>

**Chemical and photochemical characterisation of paddy-field water.** The results of the chemical characterisation of the paddy-field water samples are reported in **Table 2**. The data show low values of nitrate and nitrite and quite elevated DOC, which with appropriate substrates might produce potentially important degradation by <sup>3</sup>CDOM\* and <sup>1</sup>O<sub>2</sub>.<sup>24</sup> The Rovasenda sample was also less rich in ionic species compared to the others, possibly as a consequence of the different soil type (see SI). The fluorescence matrix (EEM) spectra (**Figure S13(SI)**) suggest the occurrence of humic materials<sup>32,34</sup> in all the investigated samples. The tentative humic abundance order Rovasenda > S.GermanoVC > Santhià is coherent with the absorption spectra, because CDOM is the main radiation absorber and humic substances are major CDOM constituents (**Figure S4(SI)**).<sup>24</sup>

The degradation of TMP (<sup>3</sup>CDOM\* probe) spiked to the water samples under study was significant under irradiation and virtually negligible in the dark (see **Figure S14(SI)**). The quantum yields of <sup>3</sup>CDOM\* formation from irradiated paddy-field water,  $\Phi_{^3\text{CDOM}^*}$ , are reported in **Table 2** together with the corresponding steady-state [<sup>3</sup>CDOM\*] values. It is  $\Phi_{^3\text{CDOM}^*} \sim 10^{-2}$ , not far from the <sup>3</sup>CDOM\* quantum yields measured upon irradiation of surface-water samples under comparable conditions.<sup>32,67</sup> The time trend of FFA (<sup>1</sup>O<sub>2</sub> probe) is reported in **Figure S14(SI)** as well. Differently from TMP, the degradation of FFA in the dark was significant in two out of three samples (Rovasenda and Santhià), thus the subtraction of the FFA transformation rate measured in the dark from that obtained under irradiation ( $R_{\text{FFA}}$ ) had a non-negligible impact on the calculation of the <sup>1</sup>O<sub>2</sub>

formation rate. The quantum yields  $\Phi_{^1O_2}$  are shown in **Table 2** and, in this case as well ( $\Phi_{^1O_2} = 10^{-3}$ - $10^{-2}$ ), they are similar to quantum yields previously measured for lake water samples under a comparable irradiation set-up.<sup>32</sup> Although our approach only measures the TMP-reactive triplet states, the fact that  $\Phi_{^1O_2} < \Phi_{^3CDOM^*}$ , with  $\Phi_{^1O_2}$  not too far from  $\Phi_{^3CDOM^*}$ , suggests an overall internal consistence of results obtained by using different probe molecules.<sup>24,32,33</sup>

The values of  $\Phi_{OH}^{CDOM}$ ,  $\bullet OH$  scavenging rate constant ( $k'_{scav}$ ) and steady-state [ $\bullet OH$ ] for the irradiated samples are reported in **Table 2** as well. The measured  $\Phi_{OH}^{CDOM}$  in the  $10^{-5}$  range is comparable to that found in irradiated surface waters.<sup>32,68,69</sup>

**PRP (photo)degradation in paddy-field water.** Water samples (20 mL) from the three paddy fields under study were spiked with  $20 \mu\text{mol L}^{-1}$  PRP and irradiated under the TL K05 lamp. Dark control experiments were also carried out. The initial PRP photodegradation rate constants are reported in **Figure 1** (error bars represent the standard error of the fit procedure). The TL K05 lamp was previously used to measure  $^3CDOM^*$ ,  $^1O_2$  and  $\bullet OH$  photoproduction, thus the values already determined of [ $\bullet OH$ ], [ $^1O_2$ ] and [ $^3CDOM^*$ ] in the same samples (see **Table 2**) are relevant to the measured PRP phototransformation. For  $CO_3^{\bullet -}$  it was assumed production by  $\bullet OH + HCO_3^- / CO_3^{2-}$  and scavenging by DOM,<sup>52,54</sup> and calculations yielded [ $CO_3^{\bullet -}$ ] =  $2.5 \cdot 10^{-17}$ ,  $3.5 \cdot 10^{-16}$  and  $1.0 \cdot 10^{-15}$  mol  $L^{-1}$  for Rovasenda, S.GermanoVC and Santhià, respectively. The modelled first-order rate constants of PRP phototransformation in each paddy-water sample were obtained as follows:

$$k_{PRP} = \frac{\Phi_{PRP} P_a^{PRP}}{[PRP]} + k_{PRP, \bullet OH} [\bullet OH] + k_{PRP, ^3CDOM^*} [^3CDOM^*] + k_{PRP, ^1O_2} [^1O_2] + k_{PRP, CO_3^{\bullet -}} [CO_3^{\bullet -}] \quad (6)$$

where  $P_a^{PRP} = \int_{\lambda} P^{\circ}(\lambda) \frac{A_{PRP}(\lambda)}{A_{CDOM}(\lambda) + A_{PRP}(\lambda)} (1 - 10^{-A_{CDOM}(\lambda) - A_{PRP}(\lambda)}) d\lambda$ . The  $^1O_2$  process was found to

be insignificant, while the modelled contributions of  $\bullet OH$ ,  $CO_3^{\bullet -}$  and direct photolysis to PRP phototransformation in irradiated paddy water are reported in **Figure 1**.



Within the uncertainty associated to experimental data and model predictions, the sum of  $\bullet\text{OH}$  and  $\text{CO}_3^{\bullet-}$  reactions and of direct photolysis could account well for the experimental phototransformation kinetics only in the case of S.GermanoVC and, more marginally, for Santhià. In the case of Rovasenda, where by the way the  $\text{CO}_3^{\bullet-}$  reactions were totally negligible, the three considered processes largely underestimated phototransformation. The  ${}^3\text{CDOM}^*$  reactions were intentionally excluded from these calculations because, when using the  $[{}^3\text{CDOM}^*]$  values obtained with the TMP probe and assuming  $k_{PRP,{}^3\text{CDOM}^*} = 10^8 \text{ L mol}^{-1} \text{ s}^{-1}$ , one predicts in all the cases a phototransformation kinetics that is around an order of magnitude faster than the experimental one. Three possible explanations can be advanced: (i) the triplet states might react fast with TMP but much more slowly or not at all with PRP, in which case the measured  $[{}^3\text{CDOM}^*]$  and/or the assumed  $k_{PRP,{}^3\text{CDOM}^*}$  might not apply to PRP photodegradation; (ii) the  $\sim 10^8 \text{ L mol}^{-1} \text{ s}^{-1}$  rate constants obtained by laser flash photolysis might considerably overestimate the actual reaction rate constants, e.g. because of physical quenching or energy dissipation; in addition or in alternative, (iii) PRP may undergo initial oxidation by reaction with  ${}^3\text{CDOM}^*$ , followed by back-reduction of partially oxidised PRP to PRP by the antioxidant moieties occurring in DOM. This back-reduction process has already been observed with several substrates and, depending on the molecule, it can be irrelevant or extremely important. Interestingly, back reduction has been excluded in the case of the  $\bullet\text{OH}$  reactions.<sup>62,63,70</sup> If  $k_{PRP,{}^3\text{CDOM}^*} < 10^8 \text{ L mol}^{-1} \text{ s}^{-1}$ , by using the TMP-derived  $[{}^3\text{CDOM}^*]$  values one can compute which values of  $k_{PRP,{}^3\text{CDOM}^*}$  would be needed to match the experimental data. For Rovasenda one gets  $k_{PRP,{}^3\text{CDOM}^*} \sim 8 \cdot 10^6 \text{ L mol}^{-1} \text{ s}^{-1}$  and, with very large error bars,  $10^6 \text{ L mol}^{-1} \text{ s}^{-1}$  for S.GermanoVC and  $10^7 \text{ L mol}^{-1} \text{ s}^{-1}$  for Santhià. Excluding the case of S.GermanoVC, it seems that  $k_{PRP,{}^3\text{CDOM}^*} \sim 10^7 \text{ L mol}^{-1} \text{ s}^{-1}$  might be used together with TMP-derived  $[{}^3\text{CDOM}^*]$  to predict PRP phototransformation. This  $k_{PRP,{}^3\text{CDOM}^*}$  value will thus be included in photochemical modelling.

The dark experiments showed an initially insignificant PRP degradation (lag phase of 10-15 hours), followed by fast transformation. The trend was comparable to that of the dark experiments reported previously, except for the shorter lag time. The latter finding is reasonable for a microbiological process, which should be easier in filtered natural waters compared to ultra-pure laboratory water. Surprisingly, degradation was eventually faster in the dark than under irradiation. The dark PRP transformation produced 34DCA with 90-100% yield (lowest for Rovasenda and highest for S.GermanoVC), while the 34DCA yield under irradiation was only 13-19% (lowest for Santhià and highest for S.GermanoVC). Considering that photochemical reactions do not appear to produce 34DCA, one has to conclude that photoinduced processes prevailed in the irradiated samples. For this to be possible (remember that PRP degradation in the dark was eventually faster than under irradiation), irradiation had to inhibit the dark PRP transformation. With the hypothesis that the dark transformation was biological (which is reasonable in the presence of a lag time), an inhibition under irradiation would not be surprising because it is well known that UV radiation inactivates microorganisms.<sup>71-74</sup> The paddy water was filtered before irradiation or dark experiments, which would eliminate part of the microorganisms. Therefore, biological processes are expected to play a more important role in pristine paddy water than in our experimental conditions.

**Modelling of PRP phototransformation.** Photochemical modelling used as input data the PRP photoreactivity parameters (**Table 1**) and absorption spectrum (see **Figure S3a(SI)**), as well as the paddy-water chemical and photochemical parameters (**Figure S4** and **Table 2**). A water depth of 5 cm was assumed, which is typical of the period of PRP application and, for the same reason, a late May - early June fair-weather sunlight was used.<sup>8</sup> Because of the large spectral overlap between the TL K05 lamp and sunlight, the quantum yields measured under the lamp were used for modelling. Based on results obtained in the previous section, we considered direct photolysis,  $\bullet\text{OH}/\text{CO}_3^{\bullet-}$  reactions, as well as triplet sensitisation with  $k_{PRP, {}^3CDOM^*} \sim 10^7 \text{ L mol}^{-1} \text{ s}^{-1}$ . To generalise on different paddy fields, a relationship was sought between the water absorption spectrum and the

DOC, as already done for surface water.<sup>52</sup> The  $A_1(\lambda) DOC^{-1}$  values of the paddy-water samples under study were very similar (see **Figure S15(SI)**), which reflects the similar values of  $SUVA_{254nm}$  (see **Table 2**). The exponential fit of the average spectrum in the 300-540 nm wavelength interval yielded  $A_1(\lambda) DOC^{-1} = (0.674 \pm 0.022) e^{-(0.013 \pm 0.001)\lambda}$ . The latter function was used to model PRP photochemistry in paddy water with varying DOC. The pre-exponential factor is slightly larger but it is of the same order of magnitude as the surface-water one, while the spectral slope ( $S = 0.013 \pm 0.001$ ) is slightly lower than that of surface waters.<sup>52</sup> Both issues suggest that paddy water may contain CDOM of comparable or slightly higher molecular weight than surface waters. An average of the experimental values was also taken for the transient formation quantum yields ( $\Phi_{OH}^{CDOM} = (1.68 \pm 0.49) \cdot 10^{-5}$ ;  $\Phi_{^3CDOM}^{CDOM} = (2.91 \pm 0.76) \cdot 10^{-2}$ ) and for the pseudo-first order  $\bullet OH$  scavenging rate constant,  $k'_{Scav} = [(1.55 \pm 0.22) \cdot 10^5 L(mg C)^{-1} s^{-1}] DOC$ . The expression of  $k'_{Scav}$  as a function of the DOC is justified by the fact that DOC measures DOM that is a major  $\bullet OH$  scavenger.<sup>24</sup> The proportionality factor  $(1.55 \pm 0.22) \cdot 10^5 L(mg C)^{-1} s^{-1}$  found here for paddy water is significantly higher than that usually found in surface waters. The elevated biological activity in flooded paddies possibly causes DOM to be continuously produced and consumed. Not having enough time to undergo phototransformation, paddy-water DOM might well be more photolabile than surface-water DOM. In fact, the latter becomes more photochemically stable when it undergoes photoprocessing in the natural environment.<sup>38,75</sup>

The PRP pseudo-first order photochemical rate constants in flooded paddy fields, modelled for mid-latitude conditions, as well as the corresponding half-life times, are reported in **Figure 2a**. It is shown that for reasonable values of the DOC (which cannot be near zero due to the presence of the rice plants), the phototransformation can approach the typical PRP lifetimes of some days<sup>8,13</sup> only for elevated values of nitrate and nitrite (nearing  $1 \text{ mmol L}^{-1}$  and  $10 \text{ } \mu\text{mol L}^{-1}$ , respectively). In the paddy fields of the present study, having  $0.1 \text{ mmol L}^{-1}$  nitrate or less and DOC above  $4 \text{ mg C L}^{-1}$ , the PRP half-life times would be longer than 20 days and could not compete with other processes

including biodegradation.<sup>8,13</sup> However, flooded paddies are very effective denitrification reactors.<sup>76,77</sup> If they were irrigated with nitrate-rich water containing around  $10^{-3}$  mol L<sup>-1</sup> nitrate (corresponding to ~15 mg N L<sup>-1</sup> or ~60 mg NO<sub>3</sub><sup>-</sup> L<sup>-1</sup>), in addition to achieving denitrification they would also divert a considerable PRP fraction away from 34DCA generation.

The direct photolysis and, at high DOC, the <sup>3</sup>CDOM\* reactions may be quite important for PRP phototransformation in the presence of low nitrate and nitrite. However, in these conditions the overall photodegradation would play a minor to negligible role in PRP attenuation. In contrast, PRP photodegradation would be important with elevated nitrate and nitrite, and in this case the <sup>•</sup>OH and CO<sub>3</sub><sup>•-</sup> processes would prevail over a wide range of DOC conditions (**Figure 2b,c**). Therefore, <sup>•</sup>OH and CO<sub>3</sub><sup>•-</sup> have a potentially elevated environmental significance in PRP phototransformation.

**Environmental implications.** Depending on the conditions, the photochemical degradation of PRP can be a competitive pathway with respect to the dark processes, possibly microbiological. The most significant photoprocesses in environmental settings are those induced by <sup>•</sup>OH and CO<sub>3</sub><sup>•-</sup>, because they would prevail with elevated nitrate and/or nitrite concentrations that make PRP photodegradation to be about as important as biotransformation. In contrast, direct photolysis and <sup>3</sup>CDOM\* reactions would prevail with low nitrate and nitrite, and in these conditions the photochemical reactions are unlikely to be important compared to the dark processes. The triplet-sensitised degradation of PRP in paddy water would be considerably slower than expected from experiments with model sensitiser. Despite the limited environmental significance of the process, further experiments will be required to elucidate this point. The photoreactions do not produce important amounts of 34DCA, while dark processes generate 34DCA with approximately quantitative yield. Elevated nitrate concentrations that enhance PRP photodegradation may occur if one wants to use flooded paddies as denitrification bioreactors, by irrigating them with water

containing elevated nitrate levels. In this case an important fraction of PRP would be degraded without producing 34DCA, thereby gaining a further advantage in addition to denitrification.

## **Acknowledgements**

DV, MM and CM acknowledge financial support by MIUR-PNRA.

## **Supporting Information available**

Additional information is available concerning studied rice fields, irradiation experiments, use of probe molecules, analytical determinations, photoreactivity measurements and dark experiments.

This material is available free of charge via the Internet at <http://pubs.acs.org>.

## **References**

- (1) Devine, M. D.; Duke, S. O.; Fedtke, C. *Physiology of Herbicide Action*. Prentice Hall, NJ, 1993.
- (2) Aldrich Material Safety Data Sheets (MSDS), last revision 2016.
- (3) Eddleston, M.; Rajapakshe, M.; Roberts, D.; Reginald, K.; Rezvi Sheriff, M. H.; Dissanayake, W.; Buckley, N. Severe propanil [N-(3,4-dichlorophenyl) propanamide] pesticide self-poisoning. *J. Toxicol Clin Toxicol.* **2002**, *40*, 847-854.
- (4) Pereira, J. L.; Antunes, S. C.; Castro, B. B.; Marques, C. R.; Gonçalves, A. M. M.; Gonçalves, F.; Pereira, R. Toxicity evaluation of three pesticides on non-target aquatic and soil organisms: commercial formulation versus active ingredient. *Ecotoxicology* **2009**, *18*, 455-463.
- (5) Okayi, R. G.; Tachia, M. U.; Ataguba, G. A.; Dikwahal, S. H. Toxicity of the herbicide propanil on *Oreochromis niloticus* fingerlings. *J. Fish. Aquat. Sci.* **2013**, *8*, 233-237.
- (6) Sancho, E.; Fernández-Vega, C.; Andreu, E.; Ferrando, M. D. Effects of propanil on the European eel *Anguilla anguilla* and post-exposure recovery using selected biomarkers as effect criteria. *Ecotoxicol. Environ. Saf.* **2009**, *72*, 704-713.

- (7) Primel, E. G.; Zanella, R.; Kurz, M. H. S.; Gonçalves, F. F.; Martins, M. L.; Machado, S. L. O.; Marchesan, E. Risk assessment of surface water contamination by herbicide residues: Monitoring of propanil degradation in irrigated rice field waters using HPLC-UV and confirmation by GC-MS. *J. Braz. Chem. Soc.* **2007**, *18*, 585-589.
- (8) Milan, M.; Vidotto, F.; Piano, S.; Negre, M.; Ferrero, A. Dissipation of propanil and 3,4-dichloroaniline in three different rice management systems. *J. Environ. Qual.* **2012**, *41*, 1487-1496.
- (9) Trubetskova, I.; Lampert, W. The juvenile growth rate of *Daphnia*: A short-term alternative to measuring the per capita rate of increase in ecotoxicology? *Arch. Environ. Contam. Toxicol.* **2002**, *42*, 193-198.
- (10) Voelker, D.; Vess, C.; Tillmann, M.; Nagel, R.; Otto, G. W.; Geisler, R.; Schirmer, K.; Scholz, S. Differential gene expression as a toxicant-sensitive endpoint in zebrafish embryos and larvae. *Aquat. Toxicol.* **2007**, *81*, 355–364.
- (11) Zhu, B.; Liu, T. Q.; Hu, X. G.; Wang, G. X. Developmental toxicity of 3,4-dichloroaniline on rare minnow (*Gobiocypris rarus*) embryos and larvae. *Chemosphere* **2013**, *90*, 1132-1139.
- (12) Marques, R.; Oehmen, A.; Carvalho, G.; Reis, M. A. M. Modelling the biodegradation kinetics of the herbicide propanil and its metabolite 3,4-dichloroaniline. *Environ. Sci. Pollut. Res.* **2015**, *22*, 6687-6695.
- (13) Santos, T. C. R.; Rocha, J. C.; Alonso, R. M.; Martinez, E.; Ibanez, C.; Barcelo, D. Rapid degradation of propanil in rice crop fields. *Environ. Sci. Technol.* **1998**, *32*, 3479-3484.
- (14) State of California, Department of pesticide regulation, PR-ENF-013a (REV. 12/08).
- (15) European Food Safety Authority (EFSA). Conclusion on the peer review of the pesticide risk assessment of the active substance propanil. *EFSA Journal* **2011**, *9*, 2085.
- (16) CCM. *Production and market of propanil in China*, 2<sup>nd</sup> edition, 2013, 47 pp.
- (17) Kanawi, E.; Van Scoy, A. R.; Budd, R.; Tjeerdema, R. S. Environmental fate and ecotoxicology of propanil: A review. *Toxicol. Environ. Chem.* **2016**, *98*, 689-704.

- (18) Moilanen, K. W.; Crosby, D. G. Photodecomposition of 3',4'-Dichloropropionanilide (Propanil). *J. Agric. Food Chem.* **1972**, *20*, 950-953.
- (19) Konstantinou, I. K.; Zarkadis, A. K.; Albanis, T. A. Photodegradation of selected herbicides in various natural waters and soils under environmental conditions. *J. Environ. Qual.* **2001**, *30*, 121-130.
- (20) Boreen, A. L.; Arnold, W. A.; McNeill, K. Photodegradation of pharmaceuticals in the aquatic environment: A review. *Aquat. Sci.* **2003**, *65*, 320-341.
- (21) Canonica, S. Oxidation of aquatic organic contaminants induced by excited triplet states. *Chimia* **2007**, *61*, 641-644.
- (22) Richard, C.; Ter Halle, A.; Sarakha, M.; Mazellier, P.; Chovelon, J. M. Solar light against pollutants. *Actual. Chim.* **2007**, *308-309*, 71-75.
- (23) Fenner, K.; Canonica, S.; Wackett, L. P.; Elsner, M. Evaluating pesticide degradation in the environment: Blind spots and emerging opportunities. *Science* **2013**, *341*, 752-758.
- (24) Vione, D.; Minella, M.; Maurino, V.; Minero, C. Indirect photochemistry in sunlit surface waters: Photoinduced production of reactive transient species. *Chemistry Eur. J.* **2014**, *20*, 10590-10606.
- (25) Sharpless, C. M. Lifetimes of triplet dissolved natural organic matter (DOM) and the effect of NaBH<sub>4</sub> reduction on singlet oxygen quantum yields: implications for DOM photophysics. *Environ. Sci. Technol.* **2012**, *46*, 4466-4473.
- (26) Marchetti, G.; Minella, M.; Maurino, V.; Minero, C.; Vione, D. Photochemical transformation of atrazine and formation of photointermediates under conditions relevant to sunlit surface waters: Laboratory measures and modelling. *Water Res.* **2013**, *47*, 6211-6222.
- (27) Buschmann, J.; Canonica, S.; Lindauer, U.; Hug, S. J.; Sigg, L. Photoirradiation of dissolved humic acid induces arsenic(III) oxidation. *Environ. Sci. Technol.* **2005**, *39*, 9541-9546.

- (28) Lancashire, P. D.; Bleiholder, H.; Van der Boom, T.; Langelüddecke, P.; Stauss, R.; Weber, E.; Witzemberger, A. A uniform decimal code for growth stages of crops and weeds. *Ann. Appl. Biol.* **1991**, *119*, 561-601.
- (29) Mack, J.; Bolton, J. R. Photochemistry of nitrite and nitrate in aqueous solution: A review. *J. Photochem. Photobiol. Chem.* **1999**, *128*, 1-13.
- (30) Bedini, A.; De Laurentiis, E.; Sur, B.; Maurino, V.; Minero, C.; Brigante, M.; Mailhot, G.; Vione, D. Phototransformation of anthraquinone-2-sulphonate in aqueous solution. *Photochem. Photobiol. Sci.* **2012**, *11*, 1445-1453.
- (31) De Laurentiis, E.; Prasse, C.; Ternes, T. A.; Minella, M.; Maurino, V.; Minero, C.; Sarakha, M.; Brigante, M.; Vione, D. Assessing the photochemical transformation pathways of acetaminophen relevant to surface waters: transformation kinetics, intermediates, and modelling. *Water Res.* **2014**, *53*, 235-248.
- (32) Marchisio, A.; Minella, M.; Maurino, V.; Minero, C.; Vione, D. Photogeneration of reactive transient species upon irradiation of natural water samples: Formation quantum yields in different spectral intervals, and implications for the photochemistry of surface waters. *Water Res.* **2015**, *73*, 145-156.
- (33) Rosario-Ortiz, F. L.; Canonica, S. Probe compounds to assess the photochemical activity of dissolved organic matter. *Environ. Sci. Technol.* **2016**, *50*, 12532-12547.
- (34) Minella, M.; Merlo, M. P.; Maurino, V.; Minero, C.; Vione, D. Transformation of 2,4,6-trimethylphenol and furfuryl alcohol, photosensitized by Aldrich humic acids subject to different filtration procedures. *Chemosphere* **2013**, *90*, 306-311.
- (35) Halladja, S.; Ter Halle, A.; Aguer, J. P.; Boulkamh, A.; Richard, C. Inhibition of humic substances mediated photooxygenation of furfuryl alcohol by 2,4,6-trimethylphenol. Evidence for reactivity of the phenol with humic triplet excited states. *Environ. Sci. Technol.* **2007**, *41*, 6066-6073.



- (36) Al Housari, F.; Vione, D.; Chiron, S.; Barbati, S. Reactive photoinduced species in estuarine waters. Characterization of hydroxyl radical, singlet oxygen and dissolved organic matter triplet state in natural oxidation processes. *Photochem. Photobiol. Sci.* **2010**, *9*, 78-86.
- (37) Canonica, S.; Freiburghaus, M. Electron-rich phenols for probing the photochemical reactivity of freshwaters. *Environ. Sci. Technol.* **2001**, *35*, 690-695.
- (38) De Laurentiis, E.; Buoso, S.; Maurino, V.; Minero, C.; Vione, D. Optical and photochemical characterization of chromophoric dissolved organic matter from lakes in Terra Nova Bay, Antarctica. Evidence of considerable photoreactivity in an extreme environment. *Environ. Sci. Technol.* **2013**, *47*, 14089-14098.
- (39) Cawley, K. M.; Korak, J. A.; Rosario-Ortiz, F. L. Quantum yields for the formation of reactive intermediates from dissolved organic matter samples from the Suwannee River. *Environ. Eng. Sci.* **2015**, *32*, 31-37.
- (40) Bodhipaksha, L. C.; Sharpless, C. M.; Chin, Y. P.; Sander, M.; Langston, W. K.; Mackay, A. A. Triplet photochemistry of effluent and natural organic matter in whole water and isolates from effluent-receiving rivers. *Environ. Sci. Technol.* **2015**, *49*, 3453-3463.
- (41) Rodgers, M. A. J.; Snowden, P. T. Lifetime of  $^1\text{O}_2$  in liquid water as determined by time-resolved infrared luminescence measurements. *J. Am. Chem. Soc.* **1982**, *104*, 5541-5543.
- (42) Wilkinson, F.; Brummer, J. Rate constants for the decay and reactions of the lowest electronically excited singlet-state of molecular oxygen in solution. *J. Phys. Chem. Ref. Data* **1981**, *10*, 809-1000.
- (43) Deister, U.; Warneck, P.; Wurzinger, C.  $\cdot\text{OH}$  radicals generated by  $\text{NO}_3^-$  photolysis in aqueous solution: Competition kinetics and a study of the reaction  $\cdot\text{OH} + \text{CH}_2(\text{OH})\text{SO}_3^-$ . *Ber. Bunsengesell. Phys. Chem.* **1990**, *94*, 594-599.
- (44) Buxton, G. V.; Greenstock, C. L.; Helman, W. P.; Ross, A. B. Critical review of rate constants for reactions of hydrated electrons, hydrogen atoms and hydroxyl radicals ( $\cdot\text{OH}/\text{O}^\cdot$ ) in aqueous solution. *J. Phys. Chem. Ref. Data* **1988**, *17*, 513-886.

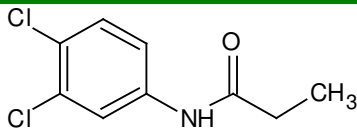
- (45) Loiselle, S. A.; Azza, N.; Cozar, A.; Bracchini, L.; Tognazzi, A.; Dattilo, A.; Rossi, C. Variability in factors causing light attenuation in Lake Victoria. *Freshwater Biol.* **2008**, *53*, 535-545.
- (46) Findlay, M.; Smoler, D. F.; Fogel, S.; Mattes, T. E. Aerobic vinyl chloride metabolism in groundwater microcosms by methanotrophic and etheneotrophic bacteria. *Environ. Sci. Technol.* **2016**, *50*, 3617-3625.
- (47) Maraccini, P. A.; Mattioli, M. C. M.; Sassoubre, L. M.; Cao, Y. P.; Griffith, J. F.; Ervin, J. S.; Van De Werfhorst, L. C.; Boehm, A. B. Solar inactivation of enterococci and *Escherichia coli* in natural waters: Effects of water absorbance and depth. *Environ. Sci. Technol.* **2016**, *50*, 5068-5076.
- (48) Kieber, R. J.; Seaton, P. J. Determination of subnanomolar concentrations of nitrite in natural waters. *Anal. Chem.* **1995**, *67*, 3261-3264.
- (49) Sur, B.; Rolle, M.; Minero, C.; Maurino, V.; Vione, D.; Brigante, M.; Mailhot, G. Formation of hydroxyl radicals by irradiated 1-nitronaphthalene (1NN): oxidation of hydroxyl ions and water by the 1NN triplet state. *Photochem. Photobiol. Sci.* **2011**, *10*, 1817-1824.
- (50) De Laurentiis, E.; Chiron, S.; Kouras-Hadef, S.; Richard, C.; Minella, M.; Maurino, V.; Minero, C.; Vione, D. Photochemical fate of carbamazepine in surface freshwaters: Laboratory measures and modeling. *Environ. Sci. Technol.* **2012**, *46*, 8164-8173.
- (51) De Laurentiis, E.; Socorro, J.; Vione, D.; Quivet, E.; Brigante, M.; Mailhot, G.; Wortham, H.; Gligorovski, S. Phototransformation of 4-phenoxyphenol sensitised by 4-carboxybenzophenone: Evidence of new photochemical pathways in the bulk aqueous phase and on the surface of aerosol deliquescent particles. *Atmos. Environ.* **2013**, *81*, 569-578.
- (52) Bodrato, M.; Vione, D. APEX (Aqueous Photochemistry of Environmentally occurring Xenobiotics): A free software tool to predict the kinetics of photochemical processes in surface waters. *Environ. Sci.: Processes Impacts* **2014**, *16*, 732-740.

- (53) Frank, R.; Klöpffer, W. Spectral solar photo irradiance in Central Europe and the adjacent north Sea. *Chemosphere* **1988**, *17*, 985-994.
- (54) Canonica, S.; Kohn, T.; Mac, M.; Real, F.J.; Wirz, J.; von Gunten, U. Photosensitizer method to determine rate constants for the reaction of carbonate radical with organic compounds. *Environ. Sci. Technol.* **2005**, *39*, 9182-9188.
- (55) Zeng, T.; Arnold, A. Pesticide photolysis in prairie potholes: Probing photosensitized processes. *Environ. Sci. Technol.* **2013**, *47*, 6735-6745.
- (56) Bianco, A.; Fabbri, D.; Minella, M.; Brigante, M.; Mailhot, G.; Maurino, V.; Minero, C.; Vione, D. Photochemical transformation of benzotriazole, relevant to sunlit surface waters: Assessing the possible role of triplet-sensitized processes. *Sci. Total Environ.* **2016**, 566-567, 712-721.
- (57) Kouras-Hadef, S.; Amine-Khodja, A.; Halladja, S.; Richard, C. Influence of humic substances on the riboflavin photosensitized transformation of 2,4,6-trimethylphenol. *J. Photochem. Photobiol. A: Chem.* **2012**, *229*, 33-38.
- (58) Wenk, J.; Eustis, S. N.; McNeill, K.; Canonica, S. Quenching of excited triplet states by dissolved natural organic matter. *Environ. Sci. Technol.* **2013**, *47*, 12802-12810.
- (59) Maddigapu, P. R.; Bedini, A.; Minero, C.; Maurino, V.; Vione, D.; Brigante, M.; Mailhot, G.; Sarakha, M. The pH-dependent photochemistry of anthraquinone-2-sulfonate. *Photochem. Photobiol. Sci.* **2010**, *9*, 323-330.
- (60) Vione, D.; De Laurentiis, E.; Berto, S.; Minero, C.; Hatipoglu, A.; Cinar, Z. Modeling the photochemical transformation of nitrobenzene under conditions relevant to sunlit surface waters: Reaction pathways and formation of intermediates. *Chemosphere* **2016**, *145*, 277-283.
- (61) Swartz, A. M.; Patton, V.; Heppleston, M. J.; Barra, M. On the photoreactivity of vitamin K compounds. *Int. J. Chem. Kinet.* **2008**, *40*, 839-844.

- (62) Wenk, J.; von Gunten, U.; Canonica, S. Effect of dissolved organic matter on the transformation of contaminants induced by excited triplet states and the hydroxyl radical. *Environ. Sci. Technol.* **2011**, *45*, 1334-1340.
- (63) Wenk, J.; Canonica, S. Phenolic antioxidants inhibit the triplet-induced transformation of anilines and sulfonamide antibiotics in aqueous solution. *Environ. Sci. Technol.* **2012**, *46*, 5455-5462.
- (64) McNeill, K.; Canonica, S. Triplet state dissolved organic matter in aquatic photochemistry: reaction mechanisms, substrate scope, and photophysical properties. *Environ. Sci. Processes Impacts* **2016**, *18*, 1381-1399.
- (65) Zhang, J.; Sun, J. Q.; Yuan, Q. Y.; Li, C.; Yan, X.; Hong, Q.; Li, S. P. Characterization of the propanil biodegradation pathway in *Sphingomonas* sp. Y57 and cloning of the propanil hydrolase gene *prpH*. *J. Haz. Mat.* **2011**, *196*, 412-419.
- (66) Herrera-González, V. E.; Ruiz-Ordaz, N.; Galíndez-Mayer, J.; Juárez-Ramírez, C.; Santoyo-Tepole, F.; Montiel, E. M. Biodegradation of the herbicide propanil, and its 3,4-dichloroaniline by-product in a continuously operated biofilm reactor. *World J. Microbiol. Biotechnol.* **2013**, *29*, 467-474.
- (67) De Laurentiis, E.; Minella, M.; Maurino, V.; Minero, C.; Brigante, M.; Mailhot, G.; Vione, D. Photochemical production of organic matter triplet states in water samples from mountain lakes, located below or above the tree line. *Chemosphere* **2012**, *88*, 1208-1213.
- (68) McCabe, A. J.; Arnold, W. A. Seasonal and spatial variabilities in the water chemistry of prairie pothole wetlands influence the photoproduction of reactive intermediates. *Chemosphere* **2016**, *155*, 640-647.
- (69) Brezonik, P. L.; Fulkerson-Brekken, J. Nitrate-induced photolysis in natural waters: Controls on concentrations of hydroxyl radical photo-intermediates by natural scavenging agents. *Environ. Sci. Technol.* **1998**, *32*, 3004-3010.

- (70) Canonica, S.; Laubscher, H. U. Inhibitory effect of dissolved organic matter on triplet-induced oxidation of aquatic contaminants. *Photochem. Photobiol. Sci.* **2008**, *7*, 547-551.
- (71) Piiparinen, J.; Enberg, S.; Rintala, J. M.; Sommaruga, R.; Majaneva, M.; Autio, R.; Vahatalo, A. V. The contribution of mycosporine-like amino acids, chromophoric dissolved organic matter and particles to the UV protection of sea-ice organisms in the Baltic Sea. *Photochem. Photobiol. Sci.* **2015**, *14*, 1025-1038.
- (72) Durif, C. M. F.; Fields, D. M.; Browman, H. I.; Shema, S. D.; Enoae, J. R.; Skiftesvik, A. B.; Bjelland, R.; Sommaruga, R.; Arts, M. T. UV radiation changes algal stoichiometry but does not have cascading effects on a marine food chain. *J. Plankton Res.* **2015**, *37*, 1120-1136.
- (73) Mostafa, S.; Rubinato, M.; Rosario-Ortiz, F. L.; Linden, K. G. Impact of light screening and photosensitization by surface water organic matter on *Enterococcus faecalis* inactivation. *Environ. Eng. Sci.* **2016**, *33*, 365-373.
- (74) Mattle, M. J.; Vione, D.; Kohn, T. Conceptual model and experimental framework to determine the contributions of direct and indirect photoreactions to the solar disinfection of MS2, phiX174, and adenovirus. *Environ. Sci. Technol.* **2015**, *49*, 334-342.
- (75) Berto, S.; Isaia, M.; Sur, B.; De Laurentiis, E.; Barsotti, F.; Buscaino, R.; Maurino, V.; Minero, C.; Vione, D. UV-vis spectral modifications of water samples under irradiation: Lake vs. subterranean water. *J. Photochem. Photobiol. A: Chem.* **2013**, *251*, 85-93.
- (76) Nakasone, H.; Kuroda, H.; Kato, T.; Tabuchi, T. Nitrogen removal from water containing high nitrate nitrogen in a paddy field (wetland). *Water Sci. Technol.* **2003**, *48*, 209-216.
- (77) Takahashi, T.; Hidehiro Inagaki, H.; Fukushima, T.; Oishi, T.; Matsuno, K. Increasing nitrate removal at low temperatures by incorporating organic matter into paddy fields. *Soil Sci. Plant Nutrit.* **2010**, *56*, 163-167.

**Table 1.** Photoreactivity parameters of PRP: direct photolysis quantum yield and second-order reaction rate constants with the main photogenerated transient species. The techniques used to determine the relevant parameters are also reported, where St.Irr. = steady irradiation and LFP = laser flash photolysis, together with the pH values used in the experiments.

		pH	Technique
	PRP		
$\Phi_{PRP}$ , unitless	0.16±0.03	6.8	St.Irr.
$k_{PRP,^{\bullet}OH}$ , L mol <sup>-1</sup> s <sup>-1</sup>	(7.0±0.5)·10 <sup>9</sup>	6.6	St.Irr.
$k_{PRP,^1O_2}$ , L mol <sup>-1</sup> s <sup>-1</sup>	(7.1±1.8)·10 <sup>4</sup>	6.7	St.Irr.
$k_{PRP,CO_3^{\bullet-}}$ , L mol <sup>-1</sup> s <sup>-1</sup> [see Reference 52]	(1.4±0.7)·10 <sup>7</sup>	8	LFP
$k_{PRP,^3AQ2S^*}$ , L mol <sup>-1</sup> s <sup>-1</sup> (reaction)	(5.0±1.1)·10 <sup>8</sup>	6.4	St.Irr.
$k_{PRP,^3AQ2S^*}$ , L mol <sup>-1</sup> s <sup>-1</sup> (quenching)	(4.6±0.4)·10 <sup>9</sup>	6.4	LFP
$k_{PRP,^31NN^*}$ , L mol <sup>-1</sup> s <sup>-1</sup> (quenching)	(3.6±0.3)·10 <sup>8</sup>	6.8	LFP
$k_{PRP,^3RF^*}$ , L mol <sup>-1</sup> s <sup>-1</sup> (quenching)	(1.3±0.3)·10 <sup>8</sup>	6.6	LFP
$k_{PRP,^3CBBP^*}$ , L mol <sup>-1</sup> s <sup>-1</sup> (quenching)	(4.9±0.9)·10 <sup>8</sup>	7.0	LFP

**Table 2.** Chemical (top) and photochemical (bottom) parameters of the paddy water samples under investigation. They were determined with the TOC analyser (TC, DOC, IC), ion chromatography (nitrate), HPLC and post-column derivatisation (nitrite), and upon sample irradiation (photochemical parameters in the lowest table section). The specific UV absorbance (SUVA<sub>254nm</sub>) is the ratio between the paddy-water absorbance at 254 nm (referred to a 1-m optical path length) and the DOC. The initial degradation rates of TMP and FFA under irradiation ( $R_{\text{TMP}}$ ,  $R_{\text{FFA}}$ ), as well as the initial formation rate of phenol from benzene ( $R_{\text{Phenol}}$ ) are reported, together with other photochemical data mentioned in the text. Additional data on water chemistry are reported in **Table S1** (SI).

<i>Sample</i>	TC, mgC L <sup>-1</sup>	DOC, mgC L <sup>-1</sup>	IC, mgC L <sup>-1</sup>	NO <sub>3</sub> <sup>-</sup> , mgN L <sup>-1</sup>	NO <sub>2</sub> <sup>-</sup> , mgN L <sup>-1</sup>	pH	SUVA <sub>254nm</sub> (L m <sup>-1</sup> mgC <sup>-1</sup> )
<b>Rovasenda</b>	15.68 ± 0.16	9.58 ± 0.17	6.09 ± 0.07	< LoD	< LoD	7.0	2.1
<b>S.Germano VC</b>	24.92 ± 0.44	6.80 ± 0.54	18.11 ± 0.31	< LoD	< LoD	8.2	2.4
<b>Santhià</b>	19.52 ± 0.35	4.84 ± 0.43	14.68 ± 0.25	1.72 ± 0.06	0.018 ± 0.003	7.7	2.4

<i>Sample</i>	$R_{\text{TMP}}$ , mol L <sup>-1</sup> s <sup>-1</sup>	$\Phi_{^3\text{CDOM}^*}$ , unitless	[ <sup>3</sup> CDOM*], mol L <sup>-1</sup>	$R_{\text{FFA}}$ , mol L <sup>-1</sup> s <sup>-1</sup>	$\Phi_{^1\text{O}_2}$ , unitless	[ <sup>1</sup> O <sub>2</sub> ], mol L <sup>-1</sup>	$R_{\text{Phenol}}$ , mol L <sup>-1</sup> s <sup>-1</sup>	$\Phi_{\cdot\text{OH}}^{\text{CDOM}}$ , unitless	$k'_{\text{Scav}}$ , s <sup>-1</sup>	[ <sup>•</sup> OH], mol L <sup>-1</sup>
<b>Rovasenda</b>	(1.34±0.10) ·10 <sup>-8</sup>	(3.63±0.12) ·10 <sup>-2</sup>	(3.33±0.03) ·10 <sup>-14</sup>	(1.47±0.27) ·10 <sup>-10</sup>	(6.96±1.47) ·10 <sup>-3</sup>	(1.27±0.24) ·10 <sup>-14</sup>	(9.41±0.62) ·10 <sup>-12</sup>	(2.93±0.27) ·10 <sup>-5</sup>	(1.36±0.09) ·10 <sup>6</sup>	(9.88±1.30) ·10 <sup>-18</sup>
<b>S.Germano VC</b>	(9.90±0.63) ·10 <sup>-9</sup>	(2.99±0.26) ·10 <sup>-2</sup>	(2.48±0.16) ·10 <sup>-14</sup>	(2.91±0.33) ·10 <sup>-10</sup>	(1.70±0.22) ·10 <sup>-2</sup>	(2.82±0.29) ·10 <sup>-14</sup>	(4.63±0.85) ·10 <sup>-12</sup>	(1.60±0.34) ·10 <sup>-5</sup>	(9.77±1.79) ·10 <sup>5</sup>	(6.77±2.48) ·10 <sup>-18</sup>
<b>Santhià</b>	(4.89±0.25) ·10 <sup>-9</sup>	(2.11±0.16) ·10 <sup>-2</sup>	(1.22±0.06) ·10 <sup>-14</sup>	(5.13±2.97) ·10 <sup>-11</sup>	(3.91±2.35) ·10 <sup>-3</sup>	(4.53±2.62) ·10 <sup>-15</sup>	(7.88±0.23) ·10 <sup>-12</sup>	(2.31±0.58) ·10 <sup>-5</sup>	(1.12±0.03) ·10 <sup>6</sup>	(1.01±0.06) ·10 <sup>-17</sup>

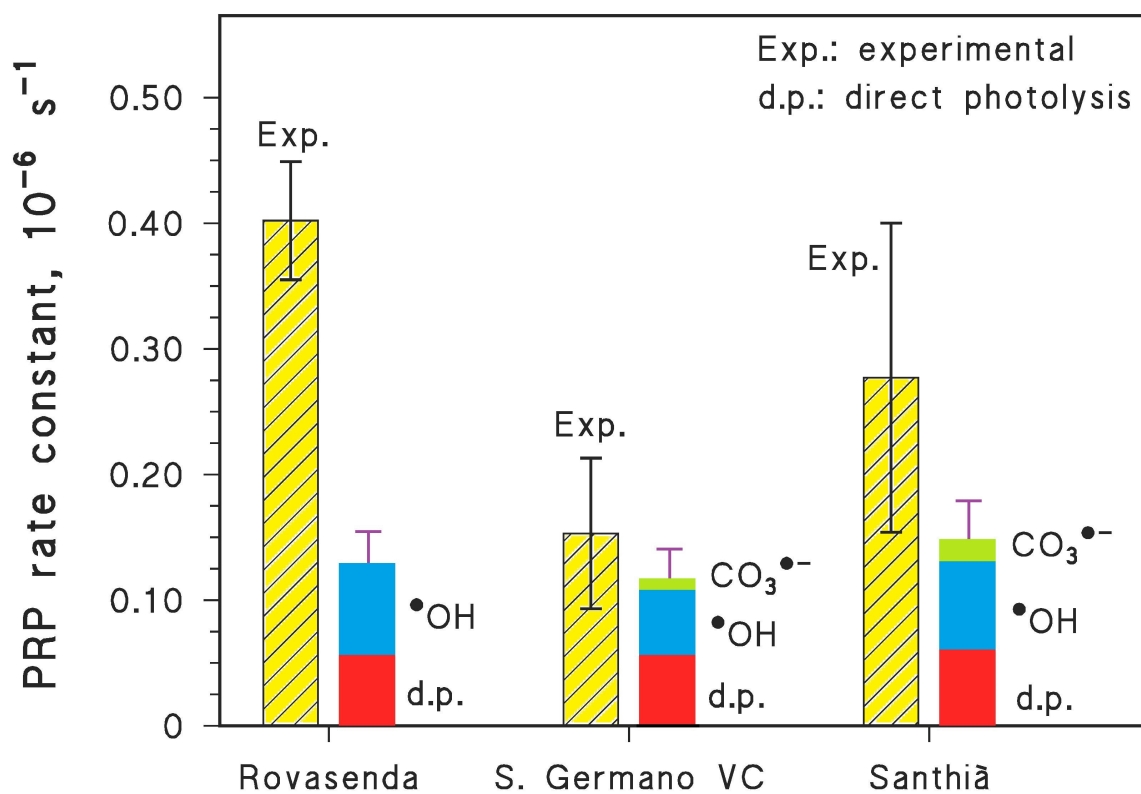


**Figure 1.** Experimental first order rate constants of PRP phototransformation in irradiated paddy water, compared to predicted rate constants of direct photolysis,  $\cdot\text{OH}$  and  $\text{CO}_3^{\cdot-}$  reactions. The error bars ( $\pm\sigma$ ) represent the uncertainties of experiments and modelling.



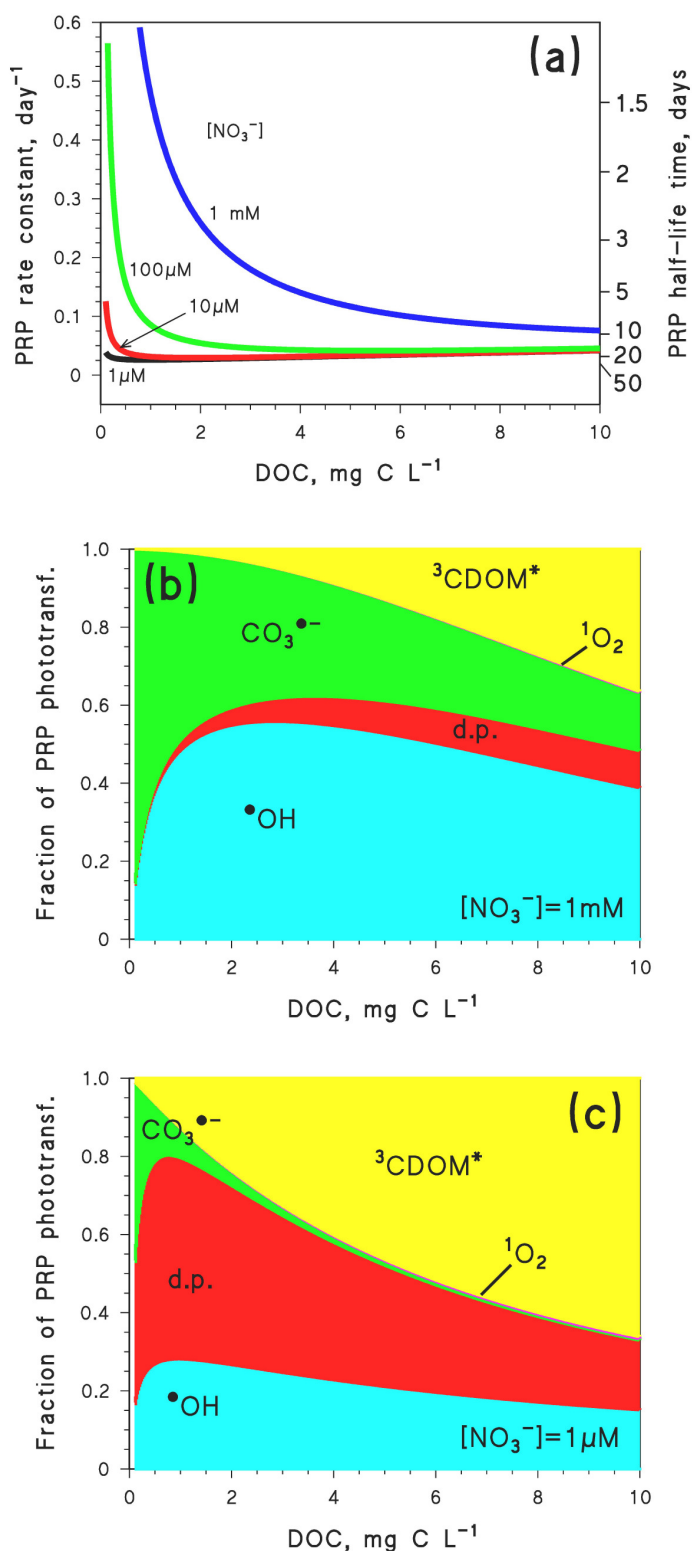


**Figure 2.** (a) APEX-modelled pseudo-first order rate constants of PRP phototransformation, and corresponding half-life times, in paddy-field water in late May-early June as a function of the DOC. (b,c) Fractions of PRP phototransformation accounted for by direct photolysis (d.p.) and  $\cdot\text{OH}/\text{CO}_3^{\cdot-}$  reactions, as a function of the DOC for nitrate concentrations of (b)  $1 \text{ mmol L}^{-1}$  and (c)  $1 \mu\text{mol L}^{-1}$ . The nitrate concentration is reported over each plot and it was assumed  $[\text{NO}_2^-] = 10^{-2} [\text{NO}_3^-]$ , which is often the case for environmental waters<sup>24</sup> and also, approximately, for the Santhià sample in this work. Other water conditions: 5 cm depth,  $1 \text{ mmol L}^{-1} \text{HCO}_3^-$ ,  $10 \mu\text{mol L}^{-1} \text{CO}_3^{2-}$ .